Elliptic flow and dissipation in heavy-ion collisions at $E_{\rm lab} \simeq (1–160)A$ GeV

Yu. B. Ivanov,[1,2,*] I. N. Mishustin,[1,2] V. N. Russkikh,[2] and L. M. Satarov[1,2]
[1]*Frankfurt Institute for Advanced Studies, J. W. Goethe Universität, D-60438 Frankfurt am Main, Germany*
[2]*The Kurchatov Institute, Moscow RU-123182, Russia*
(Received 2 August 2009; revised manuscript received 14 October 2009; published 7 December 2009)

Elliptic flow in heavy-ion collisions at incident energies $E_{\rm lab} \simeq (1–160)A$ GeV is analyzed within the model of three-fluid dynamics (3FD). We show that a simple correction factor, taking into account dissipative effects, allows us to adjust the 3FD results to experimental data. This single-parameter fit results in a good reproduction of the elliptic flow as a function of the incident energy, centrality of the collision, and rapidity. The experimental scaling of pion eccentricity-scaled elliptic flow versus charged-hadron-multiplicity density per unit transverse area also turns out to be reasonably described. Proceeding from values of the Knudsen number, deduced from this fit, we estimate the upper limit of the shear viscosity-to-entropy ratio as $\eta/s \sim 1–2$ at the CERN Super Proton Synchrotron (SPS) incident energies. This value is of the order of minimal η/s observed in water and liquid nitrogen.

DOI: 10.1103/PhysRevC.80.064904 PACS number(s): 24.10.Nz, 25.75.−q

I. INTRODUCTION

The elliptic flow (v_2) of produced particles is one of the most sensitive observables, which brings information about the degree of collectivity during the expansion stage of heavy-ion collisions [1–3]. When the collectivity is strong, such as in the case of ideal hydrodynamics, the elliptic flow takes the highest value (the so-called hydrodynamic limit). If the collectivity is weak, such as in a dilute system of weakly interacting particles, it is close to zero. Therefore, it is not surprising that v_2 is highly sensitive to dissipative effects that are associated with attenuation of the collectivity during the expansion stage. The elliptic flow turns out to be considerably reduced by the cascade "afterburner" following the hydrodynamic freeze-out [4–6] as well as by viscosity effects [7–12]. Note that the afterburner can be considered as a strong viscosity effect at the final stage of the fireball expansion.

All previously mentioned analyses of the dissipative effects were carried out for high incident energies in the BNL Relativistic Heavy-Ion Collider (RHIC) region. In this article we turn to the lower energies of the SIS-AGS-SPS (GSI Heavy-Ion Synchrotron–BNL Alternating Gradient Synchrotron–CERN Super Proton Synchrotron) region. The experimental data [13–20] in this energy region are much more fragmentary than in the RHIC domain. In the future they will essentially be complemented by new facilities, the GSI Facility for Antiproton and Ion Research (FAIR) in Darmstadt and the Nuclotron-based Ion Collider Facility (NICA) in Dubna, as well as by experiments within the low-energy-scan program at RHIC. The available data were analyzed within kinetic [21–24] and 3FD [25,26] models. It was found that the 3FD approach noticeably overestimates the data at the SPS energies independently of the stiffness of the equation of state (EoS) and stopping power used by the model. Recently, the SPS data were studied within a hybrid hydrocascade model [27] that includes afterburner effects. It was demonstrated that the afterburner indeed essentially reduces the hydrodynamic v_2 values that still, however, exceed their experimental values.

In fact, there were no studies of dissipative effects related to the elliptic flow in the AGS-SPS energy range. In this article we present such a study based on simulations within the 3FD model [25,26,28]. To estimate the dissipation, we use the approach suggested in Refs. [29–31]. We also study scaling of the elliptic flow with the midrapidity density of produced charged particles, which was experimentally revealed in Ref. [3] (see also discussion in Ref. [32]).

II. 3FD MODEL

In Ref. [28] we have introduced a three-fluid dynamical model for simulating heavy-ion collisions in the center-of-mass (c.m.) energy range $\sqrt{s_{NN}} = 2.3–30$ GeV[1] [or $E_{\rm lab} = (1–500)A$ GeV in terms of laboratory energy of the beam], which overlaps with the SIS-AGS-SPS energy range and covers the domains of future FAIR and NICA facilities. The 3FD model is a straightforward extension of the two-fluid model with radiation of direct pions [33,34] and the $(2 + 1)$-fluid model [35]. These models were extended in such a way that the created baryon-free fluid (a "fireball" fluid) is treated on equal footing with the baryon-rich fluids. For the fireball fluid we have introduced a certain formation time, during which it evolves without interaction with other fluids.

The input required by the model consists of the EoS and interfluid friction forces. Our goal is to find an EoS that is able to reproduce in the best way the largest body of available observables. The friction forces determine the stopping power of colliding nuclei and thereby the rate of thermalization of produced matter. In principle, the friction forces and the EoS are not independent, because medium modifications, providing a nontrivial EoS, also modify elementary cross

*Y.Ivanov@gsi.de

[1]The upper limit is associated with the computational demands of the 3FD code. The lower limit cuts off the region where applicability of the hydrodynamics becomes questionable.

sections. However, currently we have at our disposal only a rough estimate of the interfluid friction forces [36]. In the present version of the 3FD model these forces are fitted to the stopping power observed in proton rapidity distributions.

We have started our simulations [28] with a simple, purely hadronic EoS [37] that involves only a density-dependent mean field providing saturation of cold nuclear matter at normal nuclear density $n_0 = 0.15$ fm^{-3} with the proper binding energy -16 MeV and a certain incompressibility K. It includes 48 lowest mass hadronic states [28]. This EoS is a natural reference point for any other more elaborated EoS.

The 3FD model turns out to reasonably reproduce a great body of experimental data in a wide energy range from AGS to SPS. Figure 1 illustrates the results of Ref. [28]. Here we use the compilation [38] of experimental data from Refs. [39–44]. These data slightly differ in degree of centrality. For Au + Au collisions at AGS energies and Pb + Pb reactions at $E_{\rm lab} = 158A$ GeV, we perform our calculations taking the fixed impact parameter $b = 2$ fm. For Pb + Pb collisions at lower SPS energies, we use $b = 2.5$ fm. The overall description of the data is quite good in the whole energy range under consideration. However, a certain underestimation of the kaon yield at lower SPS energies prevents the model from reproducing the "horn" in the K^+/π^+ ratio observed experimentally in Refs. [45,46].

In the present simulations we use a slightly different set of parameters as compared with that of Ref. [28]. There are several reasons for this. We excluded all contributions of weak decays into hadronic yields, as required by the NA49 experimental data. Strong decays of baryon resonances were updated. Scalar meson $f_0(600)$ was included in the list of produced mesons. Some bugs in the code were corrected. All this inspired a refit of the model parameters. The best EoS, which reproduces the main body of experimental data, corresponds now to $K = 190$ MeV (instead of $K = 210$ MeV in Ref. [28]). In fact, the EoS's with $K = 190$ and 210 MeV are very close to each other. The enhancement factor of the friction forces estimated from the proton-proton cross sections was reduced: we take the coefficient $\beta_h = 0.5$ instead of $\beta_h = 0.75$ in Eq. (39) of Ref. [28]. With this updated set of parameters the reproduction of available data is approximately the same as in Ref. [28].

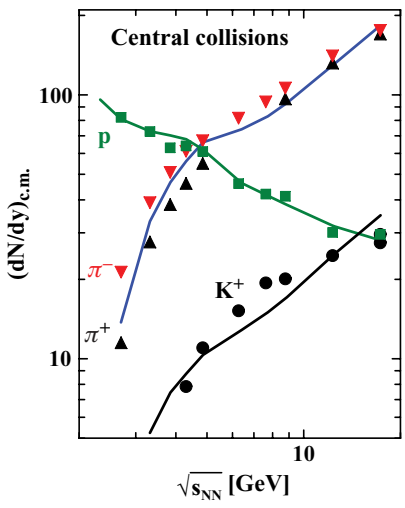

FIG. 1. (Color online) Incident energy dependence of midrapidity yield of various charged hadrons produced in central Au + Au and Pb + Pb collisions. The 3FD calculations are done with the hadronic EoS ($K = 190$ MeV). The compilation of experimental data is taken from Ref. [38].

III. ELLIPTIC FLOW

The elliptic flow, defined as $v_2 = \langle \cos 2\phi \rangle$ [2], is the second coefficient in the Fourier expansion of the azimuthal-angle[2] dependence of the single-particle distribution function of a hadronic species a, (Ed^3N_a/d^3p),

$$v_2^{(a)}(y) = \frac{\int d^2p_T \left[\left(p_x^2 - p_y^2\right)/p_T^2\right] Ed^3N_a/d^3p}{\int d^2p_T Ed^3N_a/d^3p}, \qquad (1)$$

where $\mathbf{p}_T$ is the transverse momentum of the particle; p_x and p_y are its x and y components. In calculating v_2 for pions and protons we take into account contributions of resonance decays.

Figure 2 summarizes the 3FD results [25,26,28] for the elliptic flow. The calculations were done for Au + Au collisions at $b = 6$ fm (SIS and AGS energies) and Pb + Pb collisions at $b = 5.6$ fm (SPS energies). It is seen that the proton data are well reproduced at low bombarding energies, where the squeeze-out effect dominates. The latter is caused by shadowing of expanding participant matter by spectator parts of the colliding nuclei. Note that late freeze-out turns out to be preferable for pion data at low energies, whereas the reproduction of these data is still far from perfect. At higher energies, when the standard collective mechanism of the elliptic flow formation starts to work, the 3FD model noticeably overestimates both the proton and pion data. The calculated results only weakly depend on the stiffness of the EoS. Tuning the freeze-out condition does not help very much to reduce the disagreement. The proton elliptic flow turns out to be quite insensitive to this condition. The sensitivity of the pion elliptic flow is higher. However, even very early freeze-out, which looks preferable for pions, does not allow us to fit the data. The different sensitivity of the proton and pion v_2 to the freeze-out condition is a consequence of the three-fluid nature of our model. Saturation of v_2 in the fireball fluid occurs later than that in the baryon-rich fluids. Because contribution of the fireball fluid into the pion yield is larger than for protons, the saturation of the total pion v_2 also happens later. Variation of the interfluid friction does not improve agreement with the data either, while destroying the description of other observables.

The calculations show that for $\varepsilon_{\rm frz} \lesssim 0.2$ GeV/fm^3 both the proton and pion elliptic flows stay practically unchanged. Therefore, the results obtained for $\varepsilon_{\rm frz} = 0.2$ GeV/fm^3 can be naturally associated with the hydrodynamic limit[3] of the elliptic flow.

It is natural to associate the overestimation of experimental v_2 values with dissipative effects during the expansion and

[2] ϕ is the angle with respect to the reaction plane.

[3] Note that these results correspond to the 3FD initial conditions.

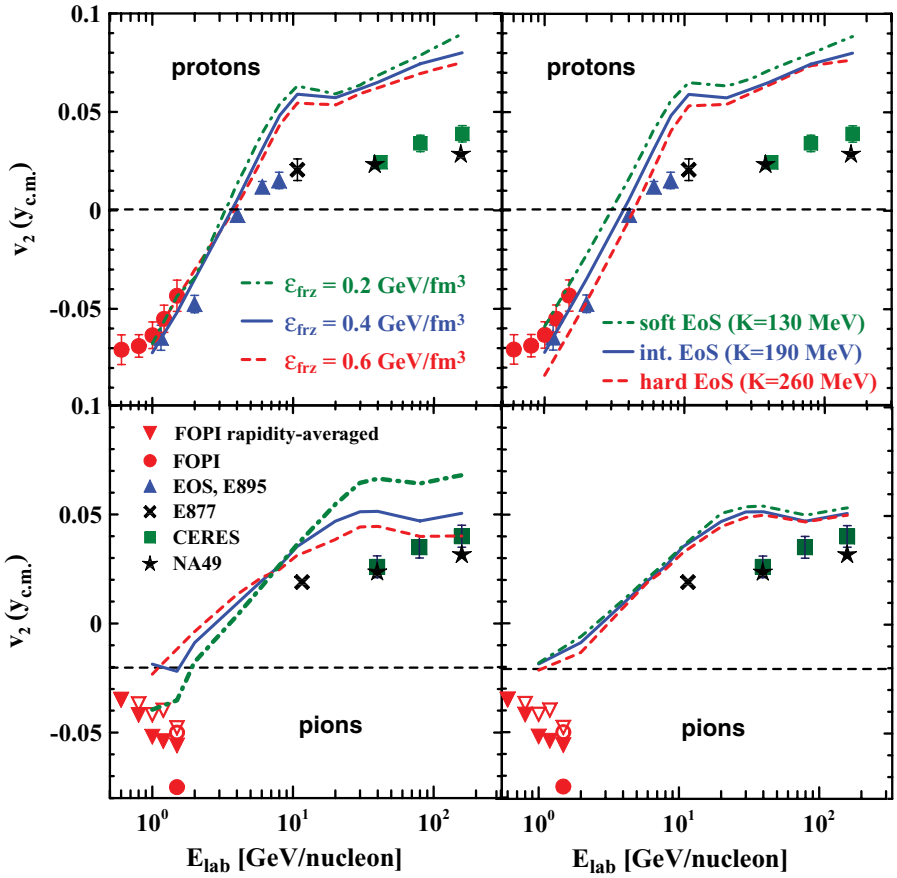

FIG. 2. (Color online) Elliptic flow of protons (top panels) and pions (bottom panels) at midrapidity as a function of incident energy in midcentral Au + Au (at SIS and AGS energies) and Pb + Pb (at SPS energies) collisions. The 3FD calculations with soft ($K = 130$ MeV), intermediate ($K = 190$ MeV), and hard ($K = 260$ MeV) EoS's at standard freeze-out energy density $\varepsilon_{frz} = 0.4\,\mathrm{GeV/fm^3}$ are displayed in the right panels. Calculations with intermediate ($K = 190$ MeV) EoS and different freeze-out energy densities $\varepsilon_{frz} = 0.2$, 0.4, and 0.6 GeV/fm^3 are presented in the left panels. Compilation of experimental data is from Ref. [15]. The FOPI pion data are from Ref. [16]. Solid symbols correspond to positive pions and open symbols correspond to negative pions; the rapidity average is taken over the interval $-1.8 < y - y_{c.m.} < 0$.

freeze-out of the participant matter. To take these effects into account we use an empirical formula suggested in Ref. [30]:

$$v_2 = \frac{v_2^{\mathrm{hydro}}}{1 + \mathrm{Kn}/\mathrm{Kn}_0}. \tag{2}$$

Here, v_2 is the observed value of the elliptic flow, v_2^{hydro} is its hydrodynamic limit, and Kn is an effective Knudsen number defined as

$$\mathrm{Kn} = \frac{\lambda}{R}, \tag{3}$$

where λ is a mean-free path of a particle and R is a characteristic size of the system (e.g., the radius of the nucleus); $\mathrm{Kn}_0 \sim 1$ is a constant. The recent transport calculation in two spatial dimensions [31] resulted in $\mathrm{Kn}_0 \simeq 0.7$. We use this value of Kn_0 for our estimates below.

As argued in Ref. [30], the Knudsen number can be represented in the form

$$\frac{1}{\mathrm{Kn}} \simeq \frac{c_s \sigma_{\mathrm{tr}}}{4S} \frac{dN_{\mathrm{tot}}}{dy}. \tag{4}$$

Here, dN_{tot}/dy is the total (charged plus neutral) hadron multiplicity per unit rapidity, which equals approximately 3/2 of the charged-hadron rapidity density dN_{ch}/dy, σ_{tr} is the transport cross section, c_s is the sound velocity in the medium, and S is the transverse overlap area between two colliding nuclei. The latter is defined as $S = \pi\sqrt{\langle x^2\rangle\langle y^2\rangle}$ [47], where $\langle x^2\rangle$ and $\langle y^2\rangle$ are mean values of x^2 and y^2 over the overlap zone[4] defined by the collision geometry.

Similarly to Ref. [29], we fit the data displayed in Fig. 2 by using Eq. (2) with Kn defined by Eq. (4) and v_2^{hydro} taken from the 3FD calculation with the late freeze-out, that is at $\varepsilon_{frz} = 0.2\ \mathrm{GeV/fm^3}$. The rapidity density dN_{ch}/dy is also calculated within the 3FD model. Note that the charged-hadron rapidity distributions are well reproduced by the 3FD model (see Fig. 1). The reduction factor $(1 + \mathrm{Kn}/\mathrm{Kn}_0)^{-1}$ is applied only at $E_{\mathrm{lab}} > 4A$ GeV because it is not justified at lower energies owing to the importance of the squeeze-out effects. Indeed, Eq. (2) was deduced from simulations of unbiased expansion of a system into the transverse directions [30]. In this case the elliptic flow can be only positive. The squeeze-out means that the transverse expansion is screened by spectators. The latter results in a suppressed and even negative elliptic flow. Therefore, at lower incident energies, purely hydrodynamical results for the late freeze-out ($\varepsilon_{frz} = 0.2\ \mathrm{GeV/fm^3}$) are presented. Probably, the elliptic flow in the squeeze-out region should be corrected for the dissipative effects but certainly not by means of Eq. (2).

The results of our fit are presented in Fig. 3. One can see that a good reproduction of the AGS and SPS data is achieved with the help of a single fitting parameter $c_s\sigma_{\mathrm{tr}} \simeq 2.3$ mb. For the midcentral collisions this leads to the estimate $\mathrm{Kn} \sim 0.7$ at

[4]We follow the conventional definition of S [47], which differs from that in Refs. [30,31] by a factor of 4.

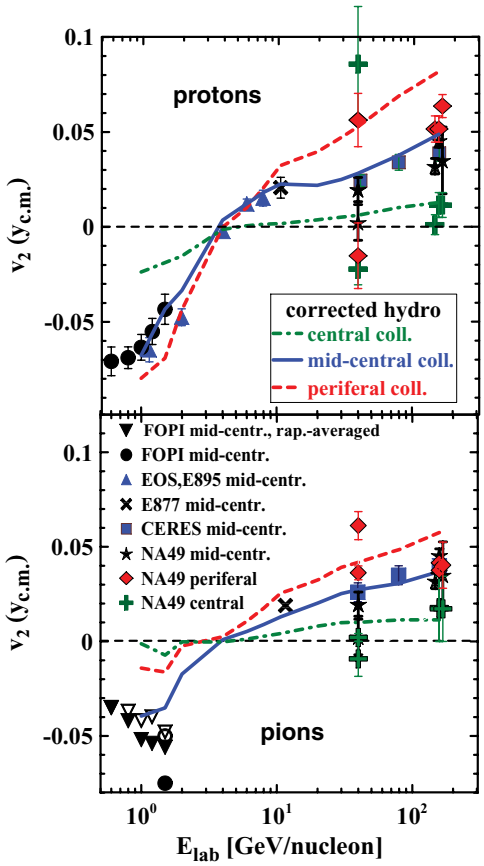

FIG. 3. (Color online) Same as Fig. 2 but for 3FD results reduced in accordance with Eqs. (2) and (4) with $c_s\sigma_{\rm tr} = 2.3$ mb. The results of 3FD calculations for the intermediate ($K = 190$ MeV) EoS and data are shown for central, midcentral, and peripheral collisions. Different experimental points (NA49) for the same incident energy and centrality correspond to different experimental methods of v_2 determination; see Ref. [19].

the midrapidity. Introduction of the dissipative correction also substantially improves the rapidity dependence of the elliptic flow. This is indeed seen from Fig. 4. Taking $c_s^2 \sim 0.15$ [48], we arrive at the estimate $\sigma_{\rm tr} \sim 6$ mb for top AGS and SPS energies. This is a surprisingly low value of the cross section. However, taking into account that $\sigma_{\rm tr}$ is the transport cross section (which is, in general, lower than the total one) and having in mind uncertainties in the Knudsen number definition (4), this value still seems to be acceptable.

Let us discuss now an approximate scaling behavior of v_2 proposed in Ref. [3]. This behavior is observed when v_2 scaled with the initial eccentricity ε is plotted as a function of $dN_{\rm ch}/dy$ scaled with the cross section of the nuclear overlap S. Both ε and S are determined by the collision geometry. In particular, ε is defined as

$$\varepsilon = \frac{\langle y^2\rangle - \langle x^2\rangle}{\langle y^2\rangle + \langle x^2\rangle}. \tag{5}$$

Below we calculate $\langle x^2\rangle$ and $\langle y^2\rangle$ with either the wounded-nucleon (WN) or the binary-collision (BC) weights; for details see Ref. [47]. These calculations are based on the usual Woods-Saxon profile of nuclear density. Within the 3FD model, the initial nuclei are represented by sharp-edged spheres. To be consistent with the model, we first calculated ε and S using the Woods-Saxon parametrization with zero diffuseness ($d = 0$) and the BC weight. The obtained results are shown in Fig. 5 by the solid lines.

Our scaling analysis is summarized in Figs. 6 and 7. First of all, we have found that there is no scaling for proton elliptic flow: points corresponding to different energies and impact parameters populate a relatively broad band rather than a universal line. This is not surprising because scaling either with the BC or WN weights is inappropriate for nucleons. Indeed, their rapidity spectra are strongly constrained by the conservation of the baryon number. As a result, contrary to pions, the number of participating nucleons is determined mainly by the initial geometry and it is not proportional to the number of binary collisions.

At the same time, the pionic v_2 exhibits an approximate scaling behavior already for pure hydrodynamic calculation (Fig. 6, top panel). This scaling is more pronounced at higher densities of charged particles, that is at higher incident energies. However, this scaling still substantially differs from the observed one (cf. experimental points in Fig. 6). When we correct the hydrodynamic results according to Eq. (2) (Fig. 6, bottom panel), the resulting v_2 reveals a scaling behavior that is closer to the experimental results. In Fig. 6 (thin lines), we also show the hydrodynamic limits of the elliptic flow. The latter results are obtained from the 3FD calculation with the late freeze-out ($\varepsilon_{\rm frz} = 0.2$ GeV/fm^3).

Although the scaling factors ε and S used in Fig. 6 [see BC ($d = 0.0$) curves in Fig. 5] are consistent with assumptions of the 3FD model, they differ from those used for scaling of the experimental data [3]. The experimental points in Figs. 6 and 7 are scaled with ε and S calculated with the WN weight and $d = 0.535$ fm [47] (see WN curves in Fig. 5). It turns out that ε and S calculated with the BC weight and $d = 0.5$ fm agree fairly well with the "experimental" scaling factors.

Upon applying the "experimental" scaling factors to the corrected elliptic flow, we obtain the scaling-like behavior displayed in Fig. 7. Here the experimental scaling turns out to be well reproduced in its high-density part, whereas the calculated elliptic flow still reveals no scaling at low charge densities. Note, however, that the lowest incident energy at which the pion elliptic flow was measured is $E_{\rm lab} = 11.5A$ GeV (the E877 data [14] in Fig. 7). If we consider v_2 only at high energies $E_{\rm lab} \gtrsim 10A$ GeV (lower bold lines in Fig. 7), the reproduction of the scaling behavior becomes much better. In principle, if we let the fitting parameter $c_s\sigma_{\rm tr}$ vary with the incident energy (i.e., smoothly join the corrected v_2 at high energies with those kept unchanged at low energies), then the scaling at $E_{\rm lab} \gtrsim 10A$ GeV can be better reproduced. However, we deliberately avoid such a multiparameter fit to keep the underlying physics more transparent.

At lower AGS energies the 3FD model certainly predicts no scaling. Apparently, this is a consequence of the partial shadowing of the transverse expansion by spectators. At lowest AGS energies this shadowing becomes dominant and leads to the negative elliptic flow.

It should be mentioned that scaling factors taking into account fluctuations of the initial eccentricity lead to a

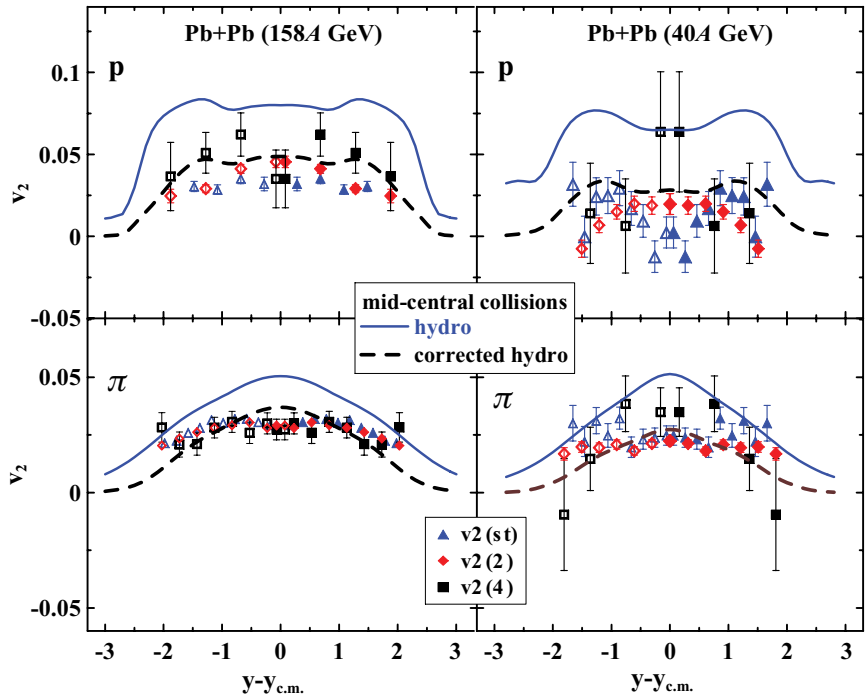

FIG. 4. (Color online) Elliptic flow of protons (top panels) and charged pions (bottom panels) in midcentral Pb + Pb collisions at $E_{\rm lab} = 158A$ GeV (left panels) and $40A$ GeV (right panels) as a function of rapidity. The 3FD calculations are performed at $b = 5.6$ fm with the intermediate EoS. Experimental data [19] obtained by different methods are displayed: by the standard method [v_2(st)] and by the method of n-particle correlations [$v_2(n)$]. Solid symbols correspond to measured data, whereas open symbols are those reflected with respect to the midrapidity. Circles in the left panels show the updated NA49 data [17] with the acceptance $0.05 < p_T < 0.35$ GeV/c for pions and $0.6 < p_T < 2.0$ GeV/c for protons.

better quality of the experimental scaling [49] (at least at RHIC energies). Because the AGS-SPS data analyzed here were obtained without applying the fluctuation corrections, we also do not use them in the scaling factors. Another aspect is the influence of initial-state fluctuations on the hydrodynamic results. In our calculation we do not introduce such fluctuations. In Ref. [50] it was shown that the initial-state fluctuations can noticeably affect the elliptic flow in semicentral collisions, especially at high transverse momenta and marginal rapidities. However, for the midrapidity region in midcentral collisions considered here, the effect of fluctuations is quite moderate.

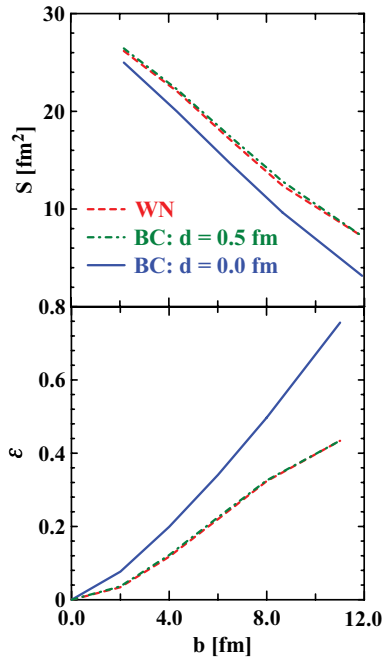

FIG. 5. (Color online) The transverse overlap area S and spatial eccentricity ε as functions of the impact parameter in Au + Au collisions for different surface diffusenesses of the Au nucleus (d) and different weights of averaging: the wounded-nucleon (WN) and the binary-collision (BC) weights [47].

IV. DISSIPATION

Having determined the effective Knudsen number, we can now estimate the role of dissipative effects during the expansion stage of a nuclear collision. Let us first attribute all this dissipation to the fluid viscosity. To estimate the latter, we use nonrelativistic formulas keeping in mind that the order of magnitude of hadronic masses is $m \sim 1$ GeV, whereas the freeze-out temperature T is of the order of 100 MeV. Note that even at the top SPS energy, where the pion yield almost twice exceeds the yield of all other particles, the system at the freeze-out stage consists mainly of heavy baryon and meson resonances that only later decay into pions. At this stage, thermal pions comprise less than 50% of all observed pions.

From the kinetic theory of simple gases one can estimate the shear viscosity coefficient as [51]

$$\eta \simeq \tfrac{1}{3}\langle p\rangle n\lambda\,, \tag{6}$$

where $\langle p\rangle \simeq \sqrt{8mT/\pi}$ is an average thermal momentum of a typical hadron, $\lambda = (n\sigma_{\rm tr})^{-1}$ is its transport mean-free path, and n is the total particle density of the medium.[5] For the rough estimate, we neglect the angular anisotropy of hadron-hadron cross sections. Taking $\sigma_{\rm tr} = 6$ mb, obtained from the fit of v_2

[5]The calculation of Ref. [52] for the hard-sphere gas gives a similar expression for η with $\sigma_{\rm tr} = 4\pi r_0^2$, where r_0 is the radius of the sphere.

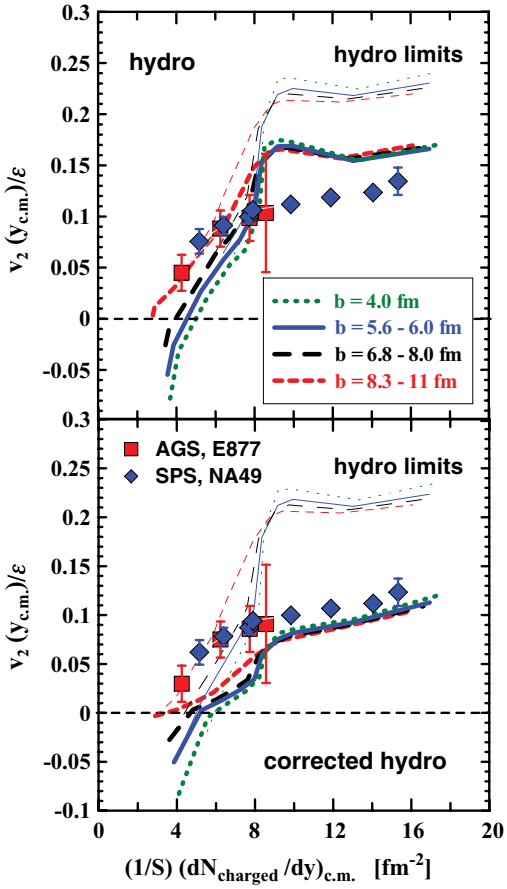

FIG. 6. (Color online) Pion elliptic flow at midrapidity divided by the eccentricity as a function of the charged-hadron rapidity density in Au + Au (AGS energies) and Pb + Pb (SPS energies) collisions at different centralities. Bold lines in the top and bottom panels display, respectively, the hydrodynamic v_2 calculated with the standard freeze-out energy density ($\varepsilon_{\rm frz} = 0.4$ GeV/fm^3) and the hydrodynamic v_2 corrected accordingly to Eq. (2). Thin lines represent the uncorrected hydrodynamic calculation with the late freeze-out ($\varepsilon_{\rm frz} = 0.2$ GeV/fm^3). The 3FD calculations were done with the intermediate EoS ($K = 190$ MeV). Compilation of experimental data is from Ref. [3].

data in Sec. III, we get the estimate

$$\eta \simeq (1.4\text{–}1.7)\ \text{fm}^{-3}, \tag{7}$$

for $T = (0.1\text{–}0.15)$ GeV. One can estimate the role of thermal pions (not hidden in resonances) by using the relativistic generalization of the previously discussed expressions suggested in Ref. [53]. The direct calculation shows that pions contribute to η not more than 30% in the same domain of T.

The relative strength of dissipative effects in fluid dynamics can be characterized by the ratio of η/s where s is the entropy density. The latter quantity can be estimated by using the Sackur-Tetrode formula [54]:

$$s = n \ln\left[\left(\frac{mT}{2\pi}\right)^{3/2}\frac{1}{n}\right] + \frac{5}{2}n. \tag{8}$$

For $T = (0.1\text{–}0.15)$ GeV and $n = 0.2$ fm^{-3} this formula leads to the estimate $s \simeq (0.6\text{–}0.7)$ fm^{-3}. The same calculation

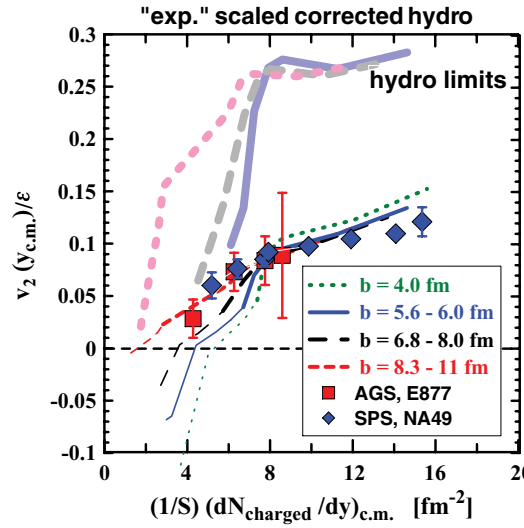

FIG. 7. (Color online) The same as in the bottom panel of Fig. 5 but scaled with "experimental" scaling quantities S and ε. Bold lines show elliptic flow at incident energies $E_{\rm lab} \geqslant 10A$ GeV; thin lines show elliptic flow at lower energies $E_{\rm lab} \leqslant 10A$ GeV.

at $n = 0.4$ fm^{-3} gives higher values $s \simeq (0.8\text{–}1.1)$ fm^{-3}. However, Eq. (8) corresponds to the gas of identical particles and, therefore, underestimates the entropy. The calculations for the gas of hadronic resonances with excluded volume corrections [55] gives entropy densities that are higher by about a factor of 2. Finally, in the considered domain of T and n we get the estimate $\eta/s \sim 1\text{–}2$. At lower incident energies, noncentral rapidities, and/or for more peripheral collisions the η/s ratio may be even higher. This is expected because the ideal hydrodynamics becomes less justified in these regions.

The obtained value of η/s is of the order of minimal values observed in water and liquid nitrogen [56]. Therefore, the strongly interacting matter in the considered energy range indeed behaves as a viscous liquid rather than a gas. However, the obtained large values of the Knudsen number Kn ~ 0.7 may be interpreted as if the fluid dynamics is not applicable at all. This would, indeed, be so if the estimated viscosity corresponded to the entire stage of the hydrodynamic expansion. In fact, the estimated Knudsen number and η/s ratio should also be attributed to the late stages of the expansion after the freeze-out (i.e., to the afterburner). During this late stage, the hydrodynamics becomes inapplicable and, hence, it is not surprising that the resulting effective Knudsen number turns out to be so large. This implies that Knudsen numbers corresponding to the hydrodynamic expansion may still be small, making hydrodynamics applicable. The argument in favor of such an interpretation is that the 3FD model is able to reproduce a large body of experimental data in the AGS-SPS energy range [28]. Another evidence in favor of this interpretation follows from the study [6,27] of a post-freeze-out evolution that has shown that the afterburner is responsible for the major part of the discrepancy between predictions of the ideal hydrodynamics and the experimental data for v_2. Therefore, these estimated values of η/s should be considered as an upper limit for the hydrodynamic expansion.

These arguments are not only relevant to the AGS-SPS energy domain. A similar analysis [29] of the PHOBOS data at RHIC energies also gives rather large values of the Knudsen number.

V. DISCUSSION AND CONCLUSIONS

In this article we have analyzed the elliptic flow in the SIS-AGS-SPS energy range within the 3FD model. Direct hydrodynamical calculations of the elliptic flow result in a good reproduction of experimental data at SIS and lower AGS energies (description of the FOPI pion data is still far from perfect), but considerably overestimate the data at the top AGS and SPS energies. The latter problem cannot be solved by either variation of the EoS stiffness or the freeze-out criterion. Changing the interfluid friction forces does not solve this problem either. In this article we attribute this problem to dissipative effects during the expansion and freeze-out stages. To estimate the role of dissipation from the difference between the 3FD results and the observed data, we apply a simple formula proposed in Ref. [30] where this difference is expressed in terms of the Knudsen number. It is shown that the interpretation of the disagreement between the 3FD model and experimental v_2 data from dissipation turns out to be fruitful. With the help of a single parameter we are able to fit the calculated v_2 values to the observed data in a broad range of incident energies, centralities, and rapidities. Moreover, the experimental scaling behavior of pion elliptic flow scaled with the initial eccentricity versus charged-hadron-multiplicity density per unit transverse area turns out to be reasonably reproduced.

Proceeding from values of the Knudsen number, deduced from the discussed fit, we estimated the viscosity-to-entropy ratio as $\eta/s \sim 1$–2. These values of η/s are of the order of minimal values observed in water and liquid nitrogen [56]. Therefore, the nuclear matter in the considered energy range indeed behaves as a liquid, however, not so perfect as at RHIC energies.

The estimated η/s ratio accumulates the effects of dissipation at the hydrodynamic expansion stage and the afterburner stage after the hydrodynamic freeze-out. Keeping in mind that the afterburner may give an important contribution to dissipation, we conclude that the estimated η/s values represent only an upper limit for this quantity when applied to the hydrodynamic expansion stage until the kinetic freeze-out. However, the authors of Ref. [53] have estimated the η/s ratios on the chemical freeze-out line observed for central collisions of heavy nuclei at beam energies from SIS to RHIC. Within the excluded-volume hadron-resonance-gas model, they found that η/s values are larger than 0.3–0.5 depending on the hard core radius. We stress that these values should be lower than ours because they correspond to the earlier chemical freeze-out stage.

Recently, the CERES collaboration reported that $\eta/s = 0.021 \pm 0.068$ at the top SPS energy [57]. This result is certainly in contradiction to our estimate of this ratio. In Ref. [57] the η/s ratio was deduced from analysis of two-pion correlation measurements, more precisely, the transverse-momentum dependence of the longitudinal pion source radius. The analysis was performed on the basis of the boost-invariant (Bjorken) solution to the relativistic viscous hydrodynamics. Concerning the latter, we should mention that it is not well justified experimentally because the pion rapidity spectra are far from being flat at SPS energies. As it is illustrated in Ref. [58], the three-fluid dynamics of the nuclear system at 158A GeV is quite different from the Bjorken picture. This could be a reason for disagreement between our results and the results of Ref. [57].

ACKNOWLEDGMENTS

We are grateful to S. Voloshin for clarifying the meaning of the elliptic-flow scaling. This work was supported in part by the Deutsche Bundesministerium für Bildung und Forschung (BMBF project RUS 08/038), the Deutsche Forschungsgemeinschaft (DFG Projects No. 436 RUS 113/957/0-1 and No. WA 431/8-1), the Russian Foundation for Basic Research (RFBR Grant No. 09-02-91331), and the Russian Ministry of Science and Education (Grant No. NS-3004.2008.2). This work was also partially supported by the Helmholtz International Center for FAIR within the framework of the LOEWE program (Landesoffensive zur Entwicklung Wissenschaftlich-Ökonomischer Exzellenz) launched by the state of Hesse.

[1] J.-Y. Ollitrault, Phys. Rev. D **46**, 229 (1992).
[2] S. Voloshin and Y. Zhang, Z. Phys. C **70**, 665 (1996); A. M. Poskanzer and S. A. Voloshin, Phys. Rev. C **58**, 1671 (1998).
[3] S. A. Voloshin and A. M. Poskanzer, Phys. Lett. **B474**, 27 (2000); S. A. Voloshin, A. M. Poskanzer, and R. Snellings, arXiv:0809.2949 [nucl-ex].
[4] D. Teaney, J. Lauret, and E. V. Shuryak, Phys. Rev. Lett. **86**, 4783 (2001).
[5] D. Teaney, Phys. Rev. C **68**, 034913 (2003).
[6] T. Hirano, U. W. Heinz, D. Kharzeev, R. Lacey, and Y. Nara, J. Phys. G **34**, S879 (2007).
[7] P. Romatschke and U. Romatschke, Phys. Rev. Lett. **99**, 172301 (2007).
[8] M. Luzum and P. Romatschke, Phys. Rev. C **78**, 034915 (2008).
[9] H. Song and U. W. Heinz, Phys. Lett. **B658**, 279 (2008).
[10] H. Song and U. W. Heinz, Phys. Rev. C **77**, 064901 (2008).
[11] K. Dusling and D. Teaney, Phys. Rev. C **77**, 034905 (2008).
[12] H. Song and U. W. Heinz, Phys. Rev. C **78**, 024902 (2008).
[13] P. Chung *et al.* (E895 Collaboration), Phys. Rev. C **66**, 021901(R) (2002).
[14] K. Filimonov *et al.* (E877 Collaboration), Nucl. Phys. **A661**, 198 (1999).
[15] A. Andronic *et al.* (FOPI Collaboration), Phys. Lett. **B612**, 173 (2005).
[16] W. Reisdorf *et al.* (FOPI Collaboration), Nucl. Phys. **A781**, 459 (2007).
[17] H. Appelshäuser *et al.* (NA49 Collaboration), Phys. Rev. Lett. **80**, 4136 (1998).

[18] H. Appelshäuser *et al.* (NA49 Collaboration), Phys. Rev. Lett. **82**, 2471 (1999).
[19] C. Alt *et al.* (NA49 Collaboration), Phys. Rev. C **68**, 034903 (2003).
[20] K. Filimonov *et al.* (CERES Collaboration), arXiv:nucl-ex/0109017; J. Slivova (CERES Collaboration), Nucl. Phys. **A715**, 615c (2003).
[21] L. V. Bravina, A. Faessler, C. Fuchs, and E. E. Zabrodin, Phys. Rev. C **61**, 064902 (2000).
[22] P. K. Sahu, W. Cassing, Nucl. Phys. **A712**, 357 (2002).
[23] M. Isse, A. Ohnishi, N. Otuka, P. K. Sahu, and Y. Nara, Phys. Rev. C **72**, 064908 (2005).
[24] H. Stöcker, E. L. Bratkovskaya, M. Bleicher, S. Soff, and Z. Zhu, J. Phys. G **31**, S929 (2005).
[25] V. N. Russkikh and Yu. B. Ivanov, Phys. Rev. C **74**, 034904 (2006).
[26] Yu. B. Ivanov and V. N. Russkikh, "What we have learned so far from 3-fluid hydrodynamics," in Proceedings of the International Workshop on Critical Point and Onset Deconfinement, Darmstadt, 2007, arXiv:0710.3708 [nucl-th].
[27] H. Petersen and M. Bleicher, Phys. Rev. C **79**, 054904 (2009).
[28] Yu. B. Ivanov, V. N. Russkikh, and V. D. Toneev, Phys. Rev. C **73**, 044904 (2006).
[29] H.-J. Drescher, A. Dumitru, C. Gombeaud, and J.-Y. Ollitrault, Phys. Rev. C **76**, 024905 (2007).
[30] R. S. Bhalerao, J.-P. Blaizot, N. Borghini, and Jean-Yves Ollitrault, Phys. Lett. **B627**, 49 (2005).
[31] C. Gombeaud and J.-Y. Ollitrault, Phys. Rev. C **77**, 054904 (2008).
[32] G. Torrieri, Phys. Rev. C **76**, 024903 (2007).
[33] I. N. Mishustin, V. N. Russkikh, and L. M. Satarov, Yad. Fiz. **48**, 711 (1988) [Sov. J. Nucl. Phys. **48**, 454 (1988)]; Nucl. Phys. **A494**, 595 (1989); Yad. Fiz. **54**, 429 (1991) [Sov. J. Nucl. Phys. **54**, 260 (1991)].
[34] V. N. Russkikh, Yu. B. Ivanov, Yu. E. Pokrovsky, and P. A. Henning, Nucl. Phys. **A572**, 749 (1994).
[35] U. Katscher, D. H. Rischke, J. A. Maruhn, W. Greiner, I. N. Mishustin, and L. M. Satarov, Z. Phys. A **346**, 209 (1993); J. Brachmann, A. Dumitru, J. A. Maruhn, H. Stöcker, W. Greiner, and D. H. Rischke, Nucl. Phys. **A619**, 391 (1997).
[36] L. M. Satarov, Yad. Fiz. **52**, 412 (1990) [Sov. J. Nucl. Phys. **52**, 264 (1990)].
[37] V. M. Galitsky and I. N. Mishustin, Sov. J. Nucl. Phys. **29**, 181 (1979).
[38] A. Andronic, P. Braun-Munzinger, and J. Stachel, Nucl. Phys. **A772**, 167 (2006).
[39] J. Barrette *et al.* (E877 Collaboration), Phys. Rev. C **51**, 3309 (1995).
[40] J. L. Klay *et al.* (E895 Collaboration), Phys. Rev. C **68**, 054905 (2003).
[41] L. Ahle *et al.* (E866 and E917 Collaboration), Phys. Lett. **B476**, 1 (2000); **B490**, 53 (2000); B. B. Back *et al.* (E917 Collaboration), Phys. Rev. Lett. **86**, 1970 (2001).
[42] S. V. Afanasiev *et al.* (NA49 Collaboration), Phys. Rev. C **66**, 054902 (2002); V. Friese *et al.* (NA49 Collaboration), J. Phys. G **30**, S119 (2004); C. Alt *et al.* (NA49 Collaboration), nucl-ex/0512033.
[43] I. G. Bearden *et al.* (NA44 Collaboration), Phys. Rev. C **66**, 044907 (2002).
[44] F. Antinori *et al.* (NA57 Collaboration), J. Phys. G **31**, 1345 (2005).
[45] M. Gaździcki and M. I. Gorenstein, Acta Phys. Pol. B **30**, 2705 (1999).
[46] M. Gaździcki, J. Phys. G **30**, S161 (2004).
[47] P. Jacobs and G. Cooper, arXiv:nucl-ex/0008015.
[48] M. Chojnacki, W. Florkowski, and T. Csörgö, Phys. Rev. C **71**, 044902 (2005).
[49] S. A. Voloshin (STAR Collaboration), J. Phys. G **34**, S883 (2007).
[50] R. P. G. Andrade *et al.*, Acta Phys. Pol. B **40**, 993 (2009).
[51] P. Danielewicz and M. Gyulassy, Phys. Rev. D **31**, 53 (1985).
[52] E. M. Lifshitz and L. P. Pitaevski, *Physical Kinetics* (Pergamon Press, Oxford, 1981).
[53] M. I. Gorenstein, M. Hauer, and O. N. Moroz, Phys. Rev. C **77**, 024911 (2008).
[54] L. D. Landau and E. M. Lifshitz, *Statistical Mechanics* (Pergamon Press, Oxford, 1986), Part 1.
[55] L. M. Satarov, M. N. Dmitriev, and I. N. Mishustin, Yad. Fiz. **72**, 1444 (2009) [Phys. Atom. Nucl. **72**, 1390 (2009)].
[56] L. P. Csernai, J. I. Kapusta, and L. D. McLerran, Phys. Rev. Lett. **97**, 152303 (2006).
[57] D. Adamova *et al.*, arXiv:0907.2799 [nucl-ex].
[58] V. N. Russkikh and Yu. B. Ivanov, Phys. Rev. C **76**, 054907 (2007).